



Published in final edited form as:

Biomacromolecules. 2012 September 10; 13(9): 2945–2951. doi:10.1021/bm300985r.

pH-Sensitive Polymeric Micelle-based pH Probe for Detecting and Imaging Acidic Biological Environments

Young Ju Lee^{†,‡,1}, Han Chang Kang^{†,§,1}, Jun Hu[†], Joseph W. Nichols^{||}, Yong Sun Jeon^{||}, and You Han Bae^{†,£,*}

[†]Department of Pharmaceutics and Pharmaceutical Chemistry, The University of Utah, 421 Wakara Way, Suite 318, Salt Lake City, UT 84108, USA

[‡]Gwangju Center, Korea Basic Science Institute, 77 Yongbong-ro, Buk-gu, Gwangju 500-757, Republic of Korea

[§]Department of Pharmacy and Integrated Research Institute of Pharmaceutical Sciences, College of Pharmacy, The Catholic University of Korea, 43 Jibong-ro, Wonmi-gu, Bucheon-si, Gyeonggi-do 420-743, Republic of Korea

^{||}Department of Bioengineering, The University of Utah, 20 S. 2030 E., Rm 108, Salt Lake City, UT 84112, USA

^{||}Department of Radiology, College of Medicine, Inha University, 7-206, 3-ga, Sinheung-dong, Jung-gu, Incheon 400-711, Republic of Korea

[£]Utah-Inha Drug Delivery Systems (DDS) and Advanced Therapeutics Research Center, 7-50 Songdo-dong, Yeonsu-gu, Incheon 406-840, Republic of Korea

Abstract

To overcome the limitations of monomeric pH probes for acidic tumor environments, this study designed a mixed micelle pH probe composed of polyethylene glycol (PEG)-*b*-poly(L-histidine) (PHis) and PEG-*b*-poly(L-lactic acid) (PLLA), which is well-known as an effective antitumor drug carrier. Unlike monomeric histidine and PHis derivatives, the mixed micelles can be structurally destabilized by changes in pH, leading to a better pH sensing system in nuclear magnetic resonance (NMR) techniques. The acidic pH-induced transformation of the mixed micelles allowed pH detection and pH mapping of 0.2–0.3 pH unit differences by pH-induced “on/off”-like sensing of NMR and magnetic resonance spectroscopy (MRS). The micellar pH probes sensed pH differences in non-biological phosphate buffer and biological buffers such as cell culture medium and rat whole blood. In addition, the pH-sensing ability of the mixed micelles was not compromised by loaded doxorubicin. In conclusion, PHis-based micelles could have potential as a tool to simultaneously treat and map the pH of solid tumors *in vivo*.

*Correspondence to: Professor You Han Bae, Department of Pharmaceutics and Pharmaceutical Chemistry, The University of Utah, 421 Wakara way, Suite 318, Salt Lake City, Utah 84108, USA, Tel: +1-801-585-1518, Fax: +1-801-585-3614., you.bae@utah.edu.

¹YJL and HCK equally contributed to this work.

Notes

The authors declare no competing financial interest.

Supporting Information Available.

Supporting information includes: details about the synthesis of PEG-PHis; TEM image of mixed micelles; NMR spectra of PEG-PHis micelles with or without PEG-PLLA in various buffer conditions. This information is available free of charge via the Internet at <http://pubs.acs.org>.

Keywords

pH imaging; poly(L-histidine); micelle pH probe; NMR; MRS

INTRODUCTION

Various tools for biomedical imaging have been developed to diagnose diseases, monitor drug delivery, and predict treatment responses.¹ pH imaging for tumor diagnosis has received particular interest due to the unique acidic environment of solid tumors resulting from its physiological and metabolic abnormality.^{2–4} Amongst the various means (such as electrodes,^{5, 6} fluorescence,⁷ luminescence,⁸ magnetic resonance (MR),^{2–4, 9, 10} and positron emission tomography (PET)^{4, 11}) which have been investigated for monitoring tumor pH *in vivo*, MR Imaging/Spectroscopy (MRI/MRS) is one of the most promising imaging techniques due to its noninvasiveness and clinical applicability.^{2–4, 9, 10} pH imaging is attainable using techniques such as pH-dependent chemical shift^{12–15} for MRS and pH-dependent relaxivity^{16–18} and pH-sensitive chemical exchange saturation transfer (CEST)^{19–21} for MRI with proper low molecular weight (MW) probes or imaging agents. However, low MW chemicals are limited in clinical applications due to their nonspecific nature, fast elimination kinetics,^{12, 22–24} and the difficulty in estimating their *in vivo* concentrations.^{2, 25}

To detect the extracellular pH (pH_e) of a tumor using MRS, pH probes should have a pK_a in the weak acidic-to-neutral pH range (pH 6.0–7.4).⁴ For this reason, low MW probes having a pH-sensitive imidazole group (*e.g.*, 2-imidazol-1-yl-3-ethoxycarbonyl-propionate^{14,15} and 2-(imidazol-1-yl) succinic acid¹²) have been applied for ¹H-MRS/MRSI-based pH measurements. In addition, Lee *et al.* recently imaged an acidic tumor or ischemic site *in vivo* using MR imaging agents (SPIO) loaded into a pH-sensitive polymeric micelle.^{26, 27}

As reported previously by our group,^{28–30} poly(ethylene glycol)-*b*-poly(L-histidine) (PEG-PHis), with or without a second polymeric component of PEG-*b*-poly(L-lactic acid) (PEG-PLLA), forms pH-sensitive micelles in basic solutions but are physically dissociated under acidic conditions. It is hypothesized that the pH-sensitive structural transition between micelles and water-soluble polymers amplify the detection of environmental pH. In addition, nanoparticles generally have greater accumulation and longer retention in solid tumors than small molecules due to the enhanced permeation and retention (EPR) effect.²³ PHis based pH-sensitive micelles can be systemically administered and are highly cytocompatible,²⁹ but when loaded with an anti-tumor chemical drug such as doxorubicin (DOX) they can effectively kill tumor cells *in vitro* and *in vivo*.²⁹

With the aforementioned attractive characteristics of PEG-PHis-based micellar constructs, this study explores their utility in pH detection and imaging. Our hypothesis was that pH-sensitive polymeric micelles at normal physiological pH (~pH 7.4) turns MR signaling from the pH-sensitive moiety (*i.e.*, imidazole groups in PHis) off, whereas acidic environments (~pH 6) will destabilize the pH-sensitive micelles, causing them to break apart into water-soluble polymers, and turn pH-sensitive MR signals on (Figure 1). Thus, in this study, we investigated whether PEG-PHis-based micelles detect and image pH in various environments such as phosphate buffer, cell culture medium and blood. In addition, we examined the micellar pH probe loaded with DOX, which can be applied for theragnosis (*i.e.*, therapy and diagnosis) in future applications.

MATERIALS AND METHODS

Materials, Cells and Rat Blood

Boc-His (Dnp)-OH-isopropanol (99%) and methoxy PEG amine hydrochloride salt (mPEG-NH₂-HCl, M_n 2 kDa) were purchased from Bachem Americas, Inc (Torrance, CA) and Jenkem Technology USA Inc. (Allen, TX), respectively. Toluene, diethyl ether, 1,4-dioxane, acetone, dimethyl sulfoxide (DMSO), *N,N'*-dimethylformamide (DMF), 2-mercaptoethanol, sodium carbonate, thionyl chloride, L-lactide, methoxy PEG-OH (mPEG-OH, M_n 2 kDa), stannous octoate, deuterium oxide (D₂O), sodium tetraborate, boric acid, 3-(trimethylsilyl) tetradeutero sodium propionate (TSP), 4-(2-hydroxyethyl)-1-piperazineethanesulfonic acid (HEPES), sodium bicarbonate, fetal bovine serum (FBS), D-glucose, penicillin-streptomycin antibiotics, RPMI1640 medium, Dulbecco's phosphate buffer solution (DPBS), ethylenediaminetetraacetic acid (EDTA), calcium hydride (CaH₂), doxorubicin (DOX), insulin, and trypsin-EDTA were bought from Sigma-Aldrich Companies (St. Louis, MO). PEG derivatives such as mPEG-OH and mPEG-NH₂ were purified by azeotropic distillation in toluene prior to use. DMF stirred in the presence of CaH₂ was distilled under reduced pressure prior to use. Other solvents and chemicals were used without further purification. Dialysis tubing with molecular weight cut-off (MWCO) of 3.5 kDa was purchased from Spectrum Laboratories, Inc. (Rancho Dominguez, CA). Rat whole blood was purchased from Innovative Research (Novi, MI).

MCF7 cells (a human breast adenocarcinoma cell line) were cultured in RPMI1640 medium supplemented with D-glucose (2 g/L), insulin (4 mg/L), and 10% FBS under humidified air containing 5% CO₂ at 37°C.

Polymer Synthesis

PEG-PHis was synthesized by a modified method with shorter steps (Figure S1) compared to that reported previously.²⁶ First, for synthesis of *N*^{im}-Dnp-histidine carboxyanhydride hydrochloride (Dnp-NCA·HCl), thionyl chloride (4 mL) was added into Boc-His(Dnp)-OH-isopropanol (4 g) in 1,4-dioxane (50 mL) under N₂ atmosphere and the reaction mixture was reacted for 1 h. Then, the precipitate was filtered and washed with dioxane and diethyl ether. Dnp-NCA·HCl was dissolved in acetone and re-purified by precipitation in diethyl ether.

Poly(*N*^{im}-Dnp-histidine) was synthesized by amine-initiated ring-opening polymerization (ROP) of Dnp-NCA·HCl. To synthesize mPEG-*b*-poly(*N*^{im}-Dnp-histidine) diblock copolymer, Dnp-NCA·HCl (4.3 g) and sodium carbonate (1.9 g) in DMF (60 mL) were stirred at room temperature (RT) for about 1 h under N₂ atmosphere. Then, mPEG-NH₂-HCl (0.75 g) in DMF (16 mL) was added into the reaction mixture. The reaction was lasted for 3 d at RT under reduced pressure and stirring. The reaction solution was poured into ethanol and re-purified by precipitation in diethyl ether. After filtration, mPEG-*b*-poly(*N*^{im}-Dnp-histidine) was dried *in vacuo*.

For PEG-PHis, Dnp deprotection of PEG-*b*-poly(*N*^{im}-Dnp-histidine) was carried out. In brief, 2-mercaptoethanol (20 mL) was added into PEG-*b*-poly(*N*^{im}-Dnp-histidine) (2.9 g) in DMSO (60 mL). The reaction solution was stirred for 12 h at RT. The solution was dialyzed against DMSO for 1 d and then against deionized water (DIW) for 2 d to remove the deprotected groups using a dialysis tube (MWCO 3.5 kDa). After lyophilization, a light yellow powder (PEG-PHis, 1.4 g) was yielded. Using ¹H-NMR spectra, MW of PHis block was estimated based on CH₂ peak of PEG for PEG-PHis.

PEG-PLLA diblock copolymer was synthesized by ROP of L-lactide initiated by the hydroxy group of mPEG-OH in the presence of the catalyst stannous octoate.³¹

Preparation of Polymeric Micelles

Polymeric micelles were constructed by using a typical diafiltration. PEG-PHIs (18 mg) with or without PEG-PLLA (2 mg) for mixed micelles or homogenous micelles, respectively, was dissolved in DMSO (5 mL). Borate buffer solution (pH 9.2, 10 mM, 1 mL) was subsequently added dropwise into the polymer solution. The resulting solution was vigorously stirred for 1 h and then transferred into a dialysis membrane (MWCO 3.5 kDa). The dialysis was performed against borate buffer (pH 9.2, 10 mM) and the buffer was replaced with fresh buffer solution at 1, 4, and 12 h. After 24 h the formed micelles were lyophilized and then reconstituted prior to use. DOX-loaded micelles were prepared similarly with dissolution of DOX at the first stage. In addition, transmission electron microscopy (TEM) observations were performed by using a Philips TECNAI T12 electron microscope. To prepare the sample, one drop of the aqueous solution was deposited onto a Formvar-carbon coated copper grid. After 5 min, the excess solution was wicked away by touching a filter paper to the edge of the grid. The sample was then observed directly by TEM without staining.

To evaluate the structural transition of the micelles in phosphate buffer, rat whole blood and cultured cells, the micelle solution (10 mg/mL) was reconstituted at pH 7.4. All pH adjustments were performed using a pH meter to monitor pH changes by adding 1N HCl into samples. For NMR measurements and MRS phantoms in phosphate buffer, the micelle solution was prepared by DPBS in D₂O and DPBS including 10% D₂O, respectively. For evaluation of micelles in rat whole blood, micelle solution prepared by DPBS in D₂O at each pH was added into the whole blood at the same pH and in the same proportions just prior to ¹H-NMR evaluation.

To monitor micelles in a culture environment of MCF7 cells, the cells were seeded on 6-well plates at 2×10^5 cells/well and cultured for 1 d. Prior to adding the micelle solution, the culture medium with serum (1 mL) was replaced with fresh culture medium (pH 6.0 and pH 7.4) without serum. The micelle solution was added into the culture medium for ¹H-NMR measurement.

¹H-NMR Experiments

¹H-NMR spectra were recorded on a Varian Unity 400 at 9 T with NaLoRAC Z-spec broadband probe for sample of DPBS in D₂O and Varian 600 with a cryoprobe to allow for bio-samples with less D₂O. TSP was used as an internal reference for ¹H chemical shifts. ¹H-NMR spectra were acquired with the following parameters at RT: acquisition time (at) of 3.2 sec, delay time (d1) of 2 sec, spectral width (sw) of 8000 Hz, and 128 averages. A pulse sequence using CPMGT2 and Presat in the VNMRJ for 600 MHz NMR (*Agilent Tech.*) was exploited for the sample of blood and MCF7 cells.

The MWs of synthesized PHIs were determined on the basis of NMR integration values with PEG with a known MW (2 kDa) used as a reference. Also, the relative integration of PHIs depending on the pH was obtained from normalization of the integration value of imidazole peaks acquired after the PEG was adjusted to have the same integration value at each pH. The integration value of the imidazole peak at pH 2.0 was used as a reference for normalization because diblock polymers can be entirely dissolved at pH 2.0. For accurate determination of the relative integration value, we delicately performed quantitative NMR experiments with enough delay time, baseline correction and internalized double references with the same quantity of TSP and DMSO. The PEG integration value did not change in any pH aqueous solution as judged by comparison with integration value of DMSO and TMS, meaning that all of the PEG forming the outer shell of the micelle is exposed to maintain a stable micelle structure. Otherwise, the integration and peak shape of PEG in micelle can be

changed if aggregation occurs during micelle preparation; similarly, PEG-PHis micelles prepared in the presence of Boc-histidine (hydrophilic small molecule), CH₂ peak in the micelle at pH 9.0 was broader and smaller compared to a soluble copolymer at pH 5.0 (Figure S3).

MRS/MRI Experiments

MRS phantom studies were conducted using a 7 T small-bore animal MRI system (BioSpec 70/30 USR, Ettlingen, Germany) with a two-turn ¹H surface coil. Point Resolved Spectroscopy (PRESS) sequence with a VAPOR sequence for water suppression was used with optimized relaxation delays. The ¹H-MRS parameters were as follows: voxel size 2.8×2.8×8 mm³, TR=1500 ms, TE=13.92 ms, and 512 averages. The phantom consisted of 5 mm NMR tubes filled with 3.8 mM mixed micelle solution at different pH values. T₁-weighted MR images were obtained using FLASH (Fast Low Angle Shot, gradient Echo pulse sequence): TR=60.2 ms, TE=15 ms, Flip Angle=30 deg, FOV= 3cm. The pixel matrix was 128 × 128. The pH values from each sample tube of the phantom were color-coded based on the H2 chemical shift using MATLAB.

RESULTS AND DISCUSSION

Although PHis-based polymers and nanoparticles have pH-sensitive characteristics such as proton buffering and structural transition,^{29, 30} their pH-sensing ability is not reported in literature. In addition, it is not known whether the imidazole groups in polymers retain the pH probing activity of monomeric imidazole groups. Thus, prior to the use of PHis-based micelles, the pH-sensitivity of PHis was first examined and compared with that of monomeric L-histidine. As shown in Figure S4, monomeric L-histidine and PHis showed similar pH sensitivity to the chemical shifts of H2 and H5 in imidazole rings, although the peaks in PHis were broader.

¹H-NMR-based pH sensing of PEG-PHis-based micelles in phosphate buffer

The aqueous solubility of PHis is decreased with increasing MW and is also pH-dependent due to different degrees of protonation of imidazole groups with varying pH. PHis homopolymers can be transformed from water-soluble polymers to hydrophobic aggregates by increasing pH. However, the formed PHis aggregates would not be appropriate for tumor applications due to their uncontrolled size distribution which can extend into the micron range. Thus, hydrophilic PEG_{2kDa} was chemically introduced into pH-sensitive PHis having different MWs (2.7 kDa ~ 4.6 kDa) to form water-soluble polymers at acidic tumor pH_e and nanosized self-assembled micelles at pH 7.4 (Figure 1(a)). Using these PEG_{2kDa}-PHis block copolymers, the MW effect of PHis on the chemical shifts of H2 and H5 in imidazole rings were evaluated by using ¹H-NMR spectra. As expected, H2 and H5 peaks in PEG_{2kDa}-PHis were shifted downfield with decreasing pH and the H2 peaks showed a more distinct pH-sensitive chemical shift change than the H5 peaks regardless of PHis's MW because the protonation at 3-N of imidazole induces an electron deshielding effect with decreasing pH (Figure 2(a) and Figure S5).

The normalized integration values of the H2 peaks in PEG_{2kDa}-PHis polymers or micelles were evaluated, accounting for the pH-induced chemical shift and molecular weight dependency of PHis. As shown in Figure 2(b), the integration values near pH 7.4 decreased with increasing MW of PHis blocks (*e.g.*, from 50% for PEG_{2kDa}-PHis_{2.7kDa} to 26% for PEG_{2kDa}-PHis_{4.6kDa}). This may occur because the longer PHis chain's increased hydrophobicity causes the PHis blocks to strongly associate in the micelle's solid core. Also, the normalized integrations of H2 peaks increased with decreasing pH (*e.g.*, for PEG_{2kDa}-PHis_{3.3kDa}, from 46% at pH 7.4 to 88% at pH 6.25) when the MW of PHis in the PEG_{2kDa}-

PHis copolymer was held constant (Figure 2(b)). The result may be from the acid-induced dissociation of the micellar structures, which expose the protonated (*i.e.*, hydrophilic) PHis blocks to the aqueous phase. These two complimentary factors improved pH sensitivity based on the normalized integration of the H2 peak. The difference between integration values at ~ pH 7.4 and ~ pH 6.3 was 47% for PEG_{2kDa}-PHis_{2.7kDa}, 42% for PEG_{2kDa}-PHis_{3.3kDa}, 37% for PEG_{2kDa}-PHis_{3.7kDa}, and 36% for PEG_{2kDa}-PHis_{4.6kDa}. However, at ~ pH 7.4 the high H2 peak's normalized integration values (25%~50%) may have been a result of the colloidal instability of PEG_{2kDa}-PHis micelles as reported previously.²⁹ This might cause an unwanted signal in normal blood pH, leading to poor resolution of tumor pH_e signal from the normal pH background.

According to our previous reports, the mixed micelles composed of PEG_{2kDa}-PHis_{5kDa} and PEG_{2kDa}-*b*-poly(L-lactic acid) (PEG_{2kDa}-PLLA_{3kDa}) are stable at pH 7.4 but unstable in the weak acidic pH range of 6.6~7.2 (which is found in the tumor extracellular space) depending on the mixing content of two block copolymers.³⁰ To increase the colloidal stability, and thus H2 peak pH sensitivity of the micelles, candidate formulations of PEG_{2kDa}-PHis_{3.3kDa} and PEG_{2kDa}-PLLA_{3kDa} were used to prepare mixed micelles for use as pH probes (Figure 1). When prepared, these micelles were spherical and monodisperse (Figure S2). The chemical shift of H2 peaks was not influenced by increasing PEG_{2kDa}-PLLA_{3kDa} content in mixed micelles (Figure S6). Interestingly, however, the H2 peak's normalized integration values of the two mixed micelles of PEG_{2kDa}-PHis_{3.3kDa} having PEG_{2kDa}-PLLA_{3kDa} (90 wt.%/10 wt.% and 80 wt.%/20 wt.%) were dramatically reduced compared with that of homomicelles of PEG_{2kDa}-PHis_{3.3kDa} (Figure 3(b)). Their reduced integration values may have resulted from the addition of PEG_{2kDa}-PLLA_{3kDa} into mixed micelles, which improved colloidal stability, and decreased the pH at which micelle destabilization occurs.³⁰ In mixed micelles made of PEG_{2kDa}-PHis_{3.3kDa} (90 wt.%) and PEG_{2kDa}-PLLA_{3kDa} (10 wt.%), the improved colloidal stability at pH 7.4 generated a large drop in the H2 peak's normalized integration value. This value could fall to as little as 12% of the value from homogenous micelles PEG_{2kDa}-PHis_{3.3kDa} (100 wt.%). Similarly, the value at pH 6.3 was 69% of the mixed micelles and 88% of the homogenous micelles. The H2 peak's integration difference ratio between pH 7.4 and pH 6.3 showed 136% better pH sensitivity for the mixed micelles than homogenous micelles. This finding indicates that the mixed micelles have great pH sensitivity. Furthermore, the mixed micelles represented the same H2 peak integration and intensity at a given pH over a 7 day colloidal stability test indicating that the pH sensitivity seems not to be changed over time (Figure S7).

¹H-NMR-based pH sensing of PEG-PHis-based micelles in cell culture medium and whole blood

PEG-PHis-based mixed micelles in phosphate buffer were chosen for the next phase of the study on the basis of its superior pH-sensing ability. A mixed micelle system composed of PEG_{2kDa}-PHis_{3.3kDa} (90 wt.%) and PEG_{2kDa}-PLLA_{3kDa} (10 wt.%) was applied to a culture medium of MCF7 cells and to rat whole blood to evaluate whether the micelle still senses pH values in biological conditions. First, the micelles were tested with cultured MCF7 cells in two different pH media (pH 6.0 and pH 7.4). ¹H-NMR experiments were performed using spinecho (CPMG2) with water suppression (Presat) within 30 min. At pH 7.4 there was almost no signal in the aromatic range, whereas the H2 peak's signal of PEG_{2kDa}-PHis_{3.3kDa} in the micelles was clearly observed at 8.25 ppm at pH 6.0 (Figure 4 and Figure S8). It is unclear whether the micelle pH probe exists in extracellular or intracellular environments because the given chemical shift of the micelle represented their average value. However, PEGylated nanoparticles are generally known to have delayed cellular uptake and improved tumor extracellular retention due to EPR and the ability of PEG-modified surfaces to resist

cell and protein binding.^{23, 32} Thus, the prompt ¹H-NMR results in our experiment most likely represent the extracellular pH.

In addition, the mixed micelles were added into rat whole blood. Like cell culture medium, almost no signal in the aromatic range was detected at pH 7.4 except the original peaks from the blood, whereas H2 and H5 signals of the mixed micelles at pH 6.0 were apparent even in whole blood including biological substances such as proteins and lipids (Figure 5 and Figure S9). Although there was a slight peak broadening in blood, the chemical shifts at pH 6.0 were almost identical to those obtained in phosphate buffer and cell culture medium. Also, most of the peaks in blood, including the mixed micelle probe, coincided with the spectrum of blood itself. This may indicate that blood components did not interact with the mixed micelles. However, some aggregates were seen in the NMR tube after several days in the refrigerator.

¹H-MRS-based pH sensing of PEG-PHis-based micelles in phosphate buffer

The findings in non-biological (*i.e.*, phosphate buffer) and biological (*i.e.*, cell culture medium and whole blood) environments showed that PEG_{2kDa}-PHis_{3.3kDa} (90 wt.%) and PEG_{2kDa}-PLLA_{3kDa} (10 wt.%) mixed micelles can be effective pH probes in ¹H-NMR, providing superior image resolution and pH sensitivity; however, ¹H-NMR is rarely used in clinical applications. ¹H-MRS, on the other hand, is much more useful in a clinical setting, meaning that a clinically useful pH probe should be effective in ¹H-MRS measurements.

The ability of the micelle probes was further evaluated by using ¹H-MRS to map pH and monitor the pH-dependent chemical shift and the intensity of the H2 peaks. MRS phantom data of the mixed micelles showed clear discrimination between pH 7.4 and pH 6.0 (Figure 6(a)) as seen in the ¹H-NMR results. In addition, the pH of phosphate buffer containing the mixed micelles was sequentially decreased by 0.2–0.3 pH units from pH 7.4 to map MRS phantoms of the mixed micelles exposed to different pH environments. As expected, ¹H-MRS of the H2 proton in the mixed micelles produced a pH map of the phantom (Figure 6(b)) and showed pH-dependent distinguishable spectra (Figure S10). The results clearly demonstrated the mixed micelles give pH-monitoring ability within acidic tumor pH ranges.

From the ¹H-MRS spectra of the micelles prepared at different pH values, the pH-dependent chemical shift and intensity changes of the H2 peaks were examined. As shown in Figure 6(c), when the mixed micelles were exposed to neutral pH conditions (pH 7.2–7.4) the H2 peak in the hydrophobic core of the micelles was not detected due to hidden PHis blocks in the micelle core; however, the H2 peak's intensity was increased with decreasing pH and a one pH unit difference between pH 7.0 and pH 6.0 caused an approximately 7-fold intensity difference. These results are consistent with the ¹H-NMR spectroscopic data.

¹H-MRS-based pH sensing of DOX-loaded PEG-PHis-based micelles in phosphate buffer

Recently, dual delivery systems using a single carrier have received attention as a tool for theragnosis.^{33, 34} The PEG-PHis-based mixed micelles proposed as an acidic pH probe in this study have been reported to be effective and biocompatible drug carriers to solid tumors^{29, 35–37}. Thus, it was investigated whether the loaded DOX can interfere with the pH sensing of PEG-PHis in the mixed micelles (composed of PEG_{2kDa}-PHis_{3.3kDa} (90 wt.%) and PEG_{2kDa}-PLLA_{3kDa} (10 wt.%)). DOX-loaded mixed micelles added into two different pH phosphate buffers (pH 6.0 and pH 7.4) showed pH-distinguishable characteristics in the aromatic range of ¹H-MRS spectra (Figure 7(a)). Like the ¹H-NMR and ¹H-MRS spectra of the mixed micelles without DOX in biological or non-biological environments, DOX-loaded mixed micelles at pH 7.4 did not show any detectable signals in the aromatic range of chemical shift, whereas at pH 6.0, the pH sensing components (*i.e.*, H2 and H5 peaks in

imidazole groups of PHis) of the micelles were clearly detectable. In addition, based on MRS spectra of the DOX-loaded mixed micelles exposed to pH 7.4 and pH 6.0, MR images were mapped and expressed as different colors (Figure 7(b)). The findings are similar to the results of the mixed micelles without DOX and indicates that DOX does not interfere with the PEG-PHis-based mixed micelle's ability to detect acidic pH.

The pH-sensing ability of the imidazole group in monomeric histidine was extended into its homopolymer (*i.e.*, PHis) and block copolymer (*i.e.*, PEG-PHis). PHis-containing micelles also recognized small differences of 0.2–0.3 pH unit based on chemical shift and integration values of pH-sensitive protons (*i.e.*, H2 and H5 of imidazole group in this study) in non-biological and biological environments. Unlike monomers, the chemical exchange processes in the polymer itself cause both peak broadening and rapid T₂ relaxation.¹³ The fact that higher pH induces shorter T₂¹³ may be advantageous because it creates a distinct difference in the MR on/off peak occurrence when using micelle pH probes. The mixed micelles are stable at normal cellular and blood pH 7.4, resulting in no ¹H-MRS detection, whereas acidic conditions destabilize the mixed micelles, leading to a strong ¹H-MRS signal. The pH-activated on-off operation of the PHis-based mixed micelles provides good pH-sensing capability and could endow high resolution diagnosis of solid tumors against a non-tumor tissue background (*i.e.*, high signal-to-noise). In addition, PEGylated micelles could improve tumor extracellular retention because PEG interferes with the cellular uptake of the micelles making the micelles highly specific to the extracellular compartment.

CONCLUSION

pH-sensitive PHis in polymers and micelles showed pH-sensing capability and was able to distinguish small pH differences in phosphate buffer, cell culture medium and rat whole blood by using MR techniques such as NMR and MRS. Therapeutic drugs in the mixed micelle pH probes did not compromise its pH-sensitivity. PHis-containing nanoparticulate drug delivery systems have great potential to be a pH sensing probe for acidic tumor environments as well as an effective therapeutic platform.

Supplementary Material

Refer to Web version on PubMed Central for supplementary material.

Acknowledgments

This study was partially supported by National Institutes of Health, USA (NIH CA101850 and CA140348).

References

1. Weissleder R, Pittet MJ. *Nature*. 2008; 452:580–9. [PubMed: 18385732]
2. Hashim AI, Zhang X, Wojtkowiak JW, Martinez GV, Gillies RJ. *NMR Biomed*. 2011; 24:582–91. [PubMed: 21387439]
3. Zhang X, Lin Y, Gillies RJ. *J Nucl Med*. 2010; 51:1167–70. [PubMed: 20660380]
4. Gallagher FA, Kettunen MI, Brindle KM. *NMR Biomed*. 2011; 24:1006–15. [PubMed: 21812047]
5. Wike-Hooley JL, Haveman J, Reinhold HS. *Radiother Oncol*. 1984; 2:343–66. [PubMed: 6097949]
6. Gerweck LE, Seetharaman K. *Cancer Res*. 1996; 56:1194–8. [PubMed: 8640796]
7. Hassan M, Riley J, Chernomordik V, Smith P, Pursley R, Lee SB, Capala J, Gandjbakhche AH. *Mol Imaging*. 2007; 6:229–36. [PubMed: 17711778]
8. Schreml S, Meier RJ, Wolfbeis OS, Landthaler M, Szeimies RM, Babilas P. *Proc Natl Acad Sci U S A*. 2011; 108:2432–7. [PubMed: 21262842]
9. Khemtong C, Kessinger CW, Gao J. *Chem Commun (Camb)*. 2009:3497–510. [PubMed: 19521593]

10. Malet-Martino M, Holzgrabe U. *J Pharm Biomed Anal.* 2011; 55:1–15. [PubMed: 21237608]
11. Vavere AL, Biddlecombe GB, Spees WM, Garbow JR, Wijesinghe D, Andreev OA, Engelman DM, Reshetnyak YK, Lewis JS. *Cancer Res.* 2009; 69:4510–6. [PubMed: 19417132]
12. Provent P, Benito M, Hiba B, Farion R, Lopez-Larrubia P, Ballesteros P, Remy C, Segebarth C, Cerdan S, Coles JA, Garcia-Martin ML. *Cancer Res.* 2007; 67:7638–45. [PubMed: 17699768]
13. van Sluis R, Bhujwalla ZM, Raghunand N, Ballesteros P, Alvarez J, Cerdan S, Galons JP, Gillies RJ. *Magn Reson Med.* 1999; 41:743–50. [PubMed: 10332850]
14. Gil S, Zaderenzo P, Cruz F, Cerdan S, Ballesteros P. *Bioorg Med Chem.* 1994; 2:305–314. [PubMed: 7922141]
15. Gil MS, Cruz F, Cerdan S, Ballesteros P. *Bioorg Med Chem Lett.* 1992; 2:1717–1722.
16. Zhang S, Wu K, Sherry AD. *Angew Chem Int Ed Engl.* 1999; 38:3192–3194. [PubMed: 10556899]
17. Lowe MP, Parker D, Reany O, Aime S, Botta M, Castellano G, Gianolio E, Pagliarin R. *J Am Chem Soc.* 2001; 123:7601–9. [PubMed: 11480981]
18. Martinez GV, Zhang X, Garcia-Martin ML, Morse DL, Woods M, Sherry AD, Gillies RJ. *NMR Biomed.* 2011; 24:1380–1391. [PubMed: 21604311]
19. Zhou J, Payen JF, Wilson DA, Traystman RJ, van Zijl PC. *Nat Med.* 2003; 9:1085–90. [PubMed: 12872167]
20. Ward KM, Balaban RS. *Magn Reson Med.* 2000; 44:799–802. [PubMed: 11064415]
21. Longo DL, Dastru W, Digilio G, Keupp J, Langereis S, Lanzardo S, Prestigio S, Steinbach O, Terreno E, Uggeri F, Aime S. *Magn Reson Med.* 2011; 65:202–11. [PubMed: 20949634]
22. Garcia-Martin ML, Herigault G, Remy C, Farion R, Ballesteros P, Coles JA, Cerdan S, Ziegler A. *Cancer Res.* 2001; 61:6524–31. [PubMed: 11522650]
23. Maeda H, Bharate GY, Daruwalla J. *Eur J Pharm Biopharm.* 2009; 71(3):409–19. [PubMed: 19070661]
24. Bae YH, Park K. *J Control Release.* 2011; 153:198–205. [PubMed: 21663778]
25. Mayr M, Burkhalter F, Bongartz G. *J Magn Reson Imaging.* 2009; 30:1289–97. [PubMed: 19937929]
26. Gao GH, Lee JW, Nguyen MK, Im GH, Yang J, Heo H, Jeon P, Park TG, Lee JH, Lee DS. *J Control Release.* 2011; 155:11–17. [PubMed: 20854855]
27. Gao GH, Im GH, Kim MS, Lee JW, Yang J, Jeon H, Lee JH, Lee DS. *Small.* 2010; 6:1201–1204. [PubMed: 20449849]
28. Lee ES, Na K, Bae YH. *J Control Release.* 2003; 91:103–113. [PubMed: 12932642]
29. Lee ES, Na K, Bae YH. *J Control Release.* 2005; 103:405–418. [PubMed: 15763623]
30. Yin H, Lee ES, Kim D, Lee KH, Oh KT, Bae YH. *J Control Release.* 2008; 126:130–8. [PubMed: 18187224]
31. Han SK, Na K, Bae YH. *Colloid Surface A Physicochem Eng Aspects.* 2003; 214:49–59.
32. Oyewumi MO, Yokel RA, Jay M, Coakley T, Mumper RJ. *J Control Release.* 2004; 95:613–626. [PubMed: 15023471]
33. Kang HC, Bae YH. *Biomaterials.* 2011; 32:4914–24. [PubMed: 21489622]
34. Yoon HY, Koo H, Choi KY, Lee SJ, Kim K, Kwon IC, Leary JF, Park K, Yuk SH, Park JH, Choi K. *Biomaterials.* 2012; 33:3980–9. [PubMed: 22364699]
35. Lee ES, Kim D, Youn YS, Oh KT, Bae YH. *Angew Chem Int Ed Engl.* 2008; 47:2418–21. [PubMed: 18236507]
36. Kim D, Lee ES, Park K, Kwon IC, Bae YH. *Pharm Res.* 2008; 25:2074–82. [PubMed: 18449626]
37. Kim D, Lee ES, Oh KT, Gao ZG, Bae YH. *Small.* 2008; 4:2043–50. [PubMed: 18949788]

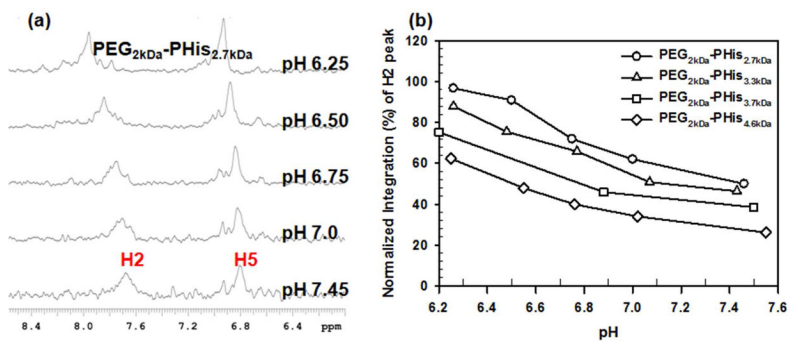


Figure 2.

(a) ¹H-NMR spectra of H2 and H5 peaks in PEG_{2kDa}-PHis_{2.7kDa} exposed at different pHs of phosphate buffer and (b) pH-dependent H2 peak's integration of PEG_{2kDa}-PHis with different MWs of PHis.

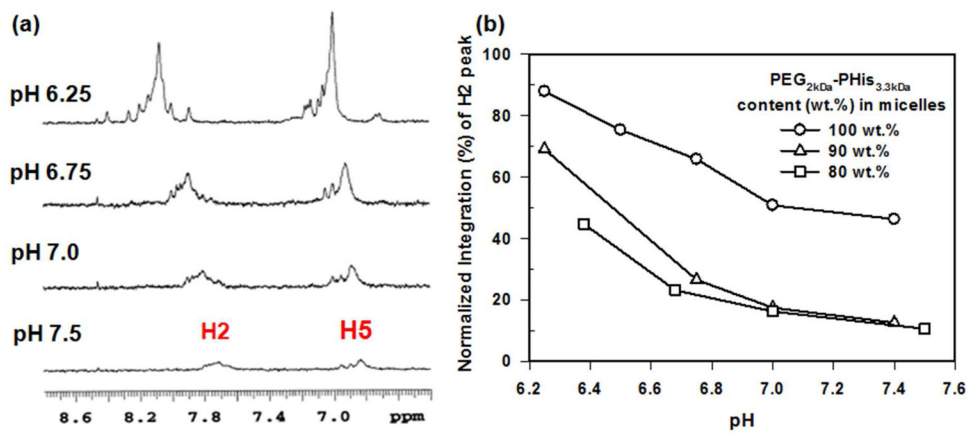


Figure 3.

(a) ¹H-NMR spectra of H2 and H5 peaks in mixed micelles of PEG_{2kDa}-PHis_{3.3kDa} (90 wt.%) having PEG_{2kDa}-PLLA_{3kDa} (10 wt.%) exposed at different pHs of phosphate buffer and (b) Comparison of pH-dependent H2 peak's integration of homogenous micelles of PEG_{2kDa}-PHis_{3.3kDa} (100 wt.%) and mixed micelles of PEG_{2kDa}-PHis_{3.3kDa} (90 wt.%) having PEG_{2kDa}-PLLA_{3kDa} (10 wt.%).

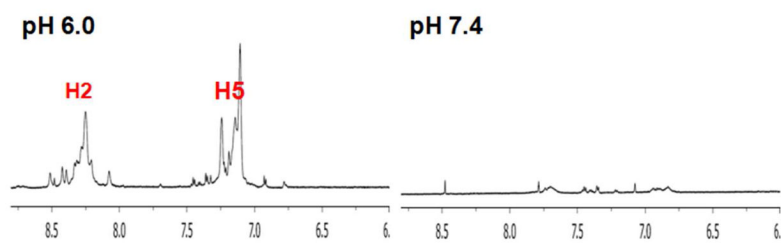


Figure 4. $^1\text{H-NMR}$ spectra of H2 and H5 peaks in mixed micelles of $\text{PEG}_{2\text{kDa}}\text{-PHis}_{3.3\text{kDa}}$ (90 wt.%) having $\text{PEG}_{2\text{kDa}}\text{-PLLA}_{3\text{kDa}}$ (10 wt.%) exposed at two different pH media (pH 6.0 and pH 7.4) of cultured MCF7 cells.

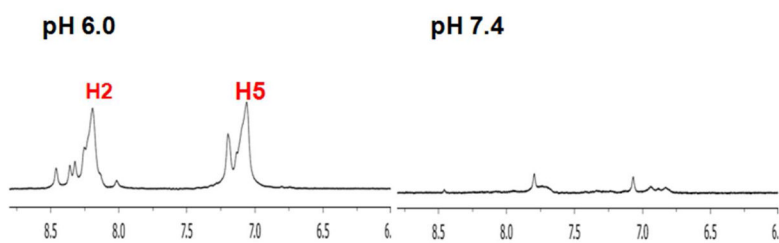


Figure 5. $^1\text{H-NMR}$ spectra of H2 and H5 peaks in mixed micelles of $\text{PEG}_{2\text{kDa}}\text{-PHis}_{3.3\text{kDa}}$ (90 wt.%) having $\text{PEG}_{2\text{kDa}}\text{-PLLA}_{3\text{kDa}}$ (10 wt.%) exposed at two different pHs (pH 7.4 and pH 6.0) of rat whole blood.

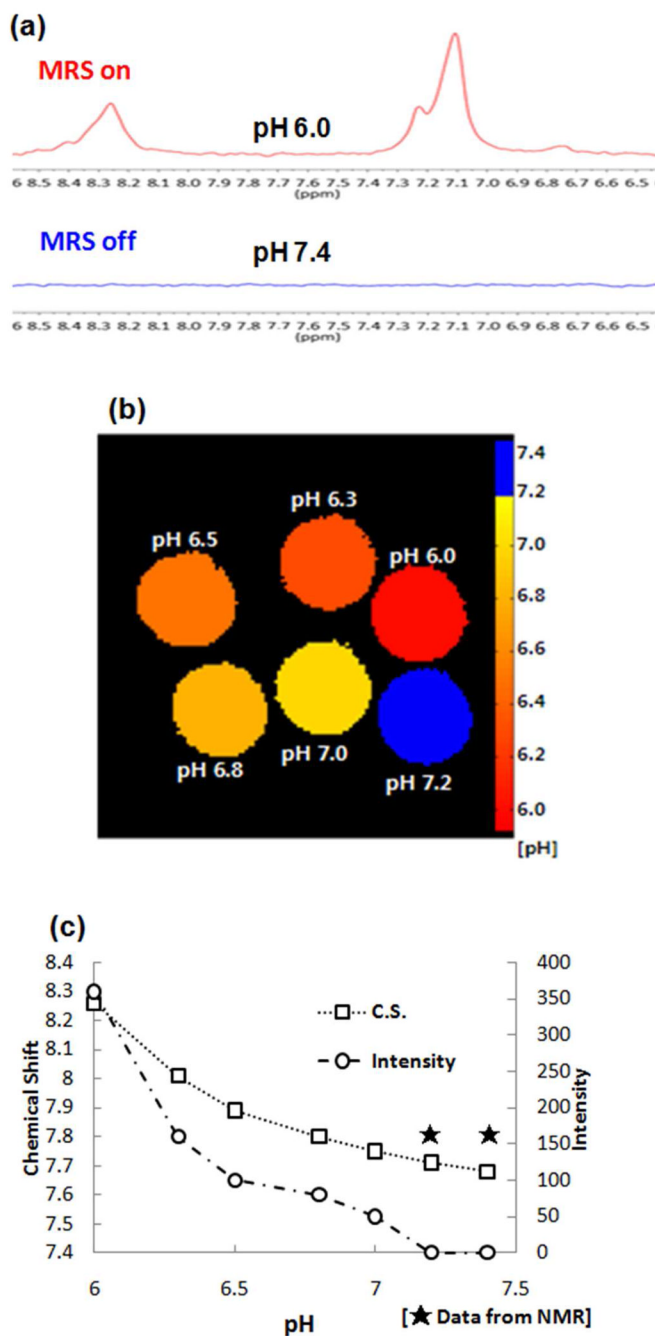


Figure 6.

(a) Phantom MRS of the mixed micelle composed of PEG_{2kDa}-PHis_{3.3kDa} (90 wt.%) and PEG_{2kDa}-PLLA (10 wt.%): Single voxel MR spectra (PRESS, TR/TE (1500/13.9 ms), nt=512, VOI 2.8×2.8×8 mm³), (b) Phantom pH map based on the chemical shift values, which was encoded as a color scale on MatLab (blue indicates that no signal was detected), and (c) pH-dependent chemical shift and intensity of H₂ peak monitored by 7.1T MRS.

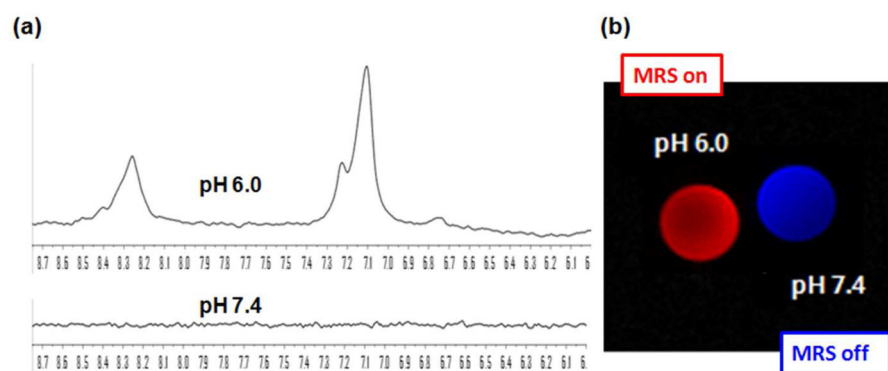


Figure 7. MRS of theragnosis-applicable Dox-loaded mixed micelle. (a) Single voxel MR spectra (PRESS, TR/TE(1500/13.9 ms), nt=512, VOI 2.8×2.8×8 mm³) and (b) MR Image colored on MatLab.